Journal of
Ceramic Science
and Technology

J. Ceram. Sci. Technol., **09** [3] 327-336 (2018)
DOI: 10.4416/JCST2018-00022
available online at: http://www.ceramic-science.com

Slurry Development for Spray Granulation of Ceramic Multicomponent Batches

P. Höhne*, B, Mieller, T. Rabe

BAM Federal Institute for Materials Research and Testing, Division 5.5 – Advanced Technical Ceramics, Unter den Eichen 44 – 46, D-12203 Berlin, Germany

received March 7, 2018; received in revised form May 16, 2018; accepted May 17, 2018

Abstract

The granules commonly yielded by spray drying procedures exhibit a hard shell and an irregular, dimpled shape, which is often described as donut-like morphology. Sintered parts produced from such granules suffer from microstructural defects and reduced mechanical properties resulting from these disadvantageous granule properties.

Using the example of alumina, zirconia and zirconia-toughened alumina (ZTA) batches, this paper shows that the morphology of the granules can be tuned by adjusting slurry stability. High zeta potential is essential to optimally disperse the particles. But to achieve spherical and soft granules the electrostatic repulsion forces between the particles should be reduced before spray granulation. Electrostatic repulsion forces were changed with the addition of nitric acid. Measurements of zeta potential and viscosity, as well as sedimentation investigations with an optical centrifuge were used for precise slurry assessment as a major precondition for optimal and reproducible adjustment of slurries before spray drying. Sedimentation analysis using an optical centrifuge was performed to investigate different influences like that of additive composition, solids content or pH-value on the sedimentation behavior. Adequately flocculated slurries lead to homogeneous, soft granules that can be easily deformed and pressed. The fraction of donut-shaped particles and the rigidity of granules were reduced. Consequently, the sintered parts produced from these granulates show improvements regarding porosity, pore size distribution, sintered density and biaxial strength.

Keywords: Slurry optimization, optical centrifugation, destabilization, spray drying, biaxial strength

I. Introduction

Powder compaction by means of uniaxial or isostatic pressing is a widely used shaping method in ceramic production, because of rapid shaping, automation, no product-drying requirement and comparatively low production cost. Dry pressing requires the use of free-flowing powders to allow rapid die filling and to avoid packing defect development. Many powders, because of their small size, irregular shape or surface characteristics, are cohesive and do not flow well. Hence, granulation methods are used to transform fine raw material to coarser granules. Such granules have a larger size and more spherical shape than initial powder particles. Both are contributing factors and their modification improves the flow properties. The ideal granule for dry-pressing should be spherical with a diameter of about 50 to 100 µm, ensuring good flowability [1].

Different granulation methods are competing in powder metallurgy and ceramics [2,3]. Starting from a slurry, spray drying, fluidized bed techniques and (spray) freeze granulation are available. Furthermore, granulates may be formed by the appropriate admixing of a binder solution and other organic additives into a stirred dry powder, that is pelletization.

Spray-drying granulation appears to be the best method for obtaining granules with high flowability on industrial scale. But strength-reducing internal microstructural defects caused by spray-dried granules with hollow and hard shells are often observed in compacted green and sintered ceramics. Hence, the characteristics of the granules have to be optimized for better compaction behavior and a reduced number and size of flaws in the powder compact.

Many authors have extensively studied and described typical microstructural defects[4–6] caused by spray-dried granules. Two defect categories are described in the literature [4], round-shaped large pores resulting from hollows or dimples in the granules and crack-like porosities. Both defect types originate from an incomplete destruction of granules under compaction pressure.

To understand this behavior of granules, a detailed consideration of the spray-drying process is helpful. The spray-drying process uses a ceramic suspension, which is a mixture of a liquid carrier phase and the solid ceramic particles suspended within. Depending on different parameters such as dispersant content and pH-value, the solid particles are either well dispersed or agglomerated. Two sequential steps have to be controlled in the process of granulate formation: atomization and droplet drying [5]. In the two-fluid nozzle, the relative velocity between the liquid and gas is the main driving force of the atomization process and is controlled by nozzle geometry and rates of liquid feed and atomization gas flow. Droplets injected

* Corresponding author: patrick.hoehne@bam.de

into a spray-dryer chamber dry as a result of the evaporation of water from the surface. Hard granules with hollows arise when well-dispersed feed slurries are used. This phenomenon originates from the fast particle and binder migration to the periphery, as droplet drying proceeds. A dense dried layer forms instantaneously at the droplet surface. Another typical source of flaws in dry-pressed parts is the incomplete cohesion of granules, which can lead to crack-like defects at the granule boundaries. This behavior has been imputed to an uneven distribution of the binder in the pressed bodies, caused by its migration toward the granule surface during drying [6,7]. Hence, the interparticle forces, which are responsible for the suspension stability (dispersed or destabilized), play an important role in the evaluation of the granule morphology.

Interparticle forces and resultant granules properties can be effectively manipulated by adapting the properties of the slurry, especially the level of flocculation, as will be demonstrated in this paper. A link between formation of hollow granules and level of flocculation of the slurry was for the first time discussed by Lee *et al.* [8]. They have found that homogeneous granules form at low dispersant levels for non-aqueous silicon nitride slurries with PVB binder and PEG plasticizer, but hollow granules form when a high dispersant level is used. They have also found that the particle-packing density in homogeneous granules is lower than in the hollow granules. Takahashi *et al.* [9] have reported similar results in aqueous silicon nitride slurries when the level of flocculation is controlled by varying the slurry pH-value. The pH-dependent zeta potential controls the slurry flocculation through its dominant effect on the electrostatic repulsion between the particles. To avoid particle migration during the drying step, they suggest the use of slightly flocculated slurries.

Subsequent investigations confirmed that the flocculation level of a slurry has a major influence on the final granule properties also in the case of using other ceramic raw materials, as alumina [10,11,12], zirconia [13], and ceramic composites [14,15,16]. Nevertheless, even now many sintered components produced from commercially available granules contain typical microstructural defects caused by unsuitable granule properties.

Although several investigations prove the reduction or prevention of dimpled, hard-shelled hollow granules with the use of flocculated slurries, little attention has been paid to the final properties of sintered ceramics. Therefore, a systematic investigation of alumina, zirconia and zirconia-toughened alumina (ZTA) batches was conducted. Dispersed and flocculated slurries were developed and spray-dried with a two-fluid nozzle in a lab spray dryer under identical conditions. Properties of granules, pressed and sintered bodies are compared to demonstrate the effect and potential of slurry optimization.

Furthermore, this paper presents for the first time the optical centrifuge as a characterization tool for slurries used in spray granulation. The turbidity of a sedimenting slurry can thereby be measured as a function of time and position in the cuvette. With 2500 detectors distributed over the cuvette height, a high spatial resolution regarding transmission behavior is possible. Each recorded transmission profile consists of numerous individual transmission values. At a user-defined time interval, the transmission of all detectors is measured at once, delivering a transmission profile for this specific time over the whole cuvette height. This allows the detection of minor changes in turbidity anywhere within the slurry height. Fig. 1 shows a typical transmission diagram of an 80 wt% alumina slurry measured with the centrifuge. Values that can be extracted from such measurement are, for example, the sediment height (indicator of the packing density), the sedimentation rate (measured by the distance between successively recorded transmission profiles), and the slope of the transmission profiles. The sediment height is assessed relatively, because the filling height shows small differences that need to be considered. The relative sediment height (RSH) is calculated using the following formula (1):

$$\mathrm{RSH} = \frac{h_{\mathrm{sed}}}{h_{\mathrm{men}}} \tag{1}$$

With subscripts indicating the extracted values with h_{sed} for the sediment height and h_{men} the height of the meniscus (corresponds to the filling height). The slope of the transmission profile is an indicator of the particle size distribution. The smaller the slope the more expanded is the sedimentation front since larger particles sediment faster, leaving behind smaller particles which slightly affect the transmission. In contrast, a nearly vertical transmission profile indicates a well-defined sharp front which comes from either a very narrow particle size distribution or an established particle network structure in the slurry. Further information is provided by the distance between the transmission profiles. A fixed time between each transmission measurement is set. So, the distance between successive transmission profiles can be used to calculate the sedimentation rate of the particles. The sedimentation rate and the final relative sediment height are useful for evaluating the stability of a suspension. A low sedimentation rate, indicated by narrow spaces between adjacent transmission profiles, is desired. Furthermore, a low sediment height is desired, which correlates to individual sedimentation of each particle, allowing close packing. The possibility to simultaneously measure the transmission over the whole cuvette height in a user-defined time interval and user-defined centrifugation force allows a more precise slurry characterization than conventional setups, where turbidity is measured at a fixed height in the cuvette.

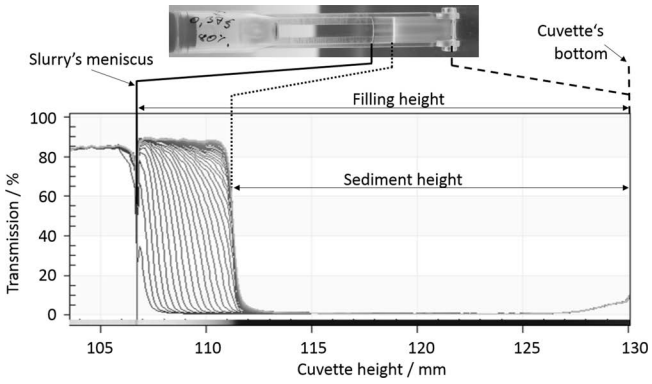

Fig. 1: Evolution of transmission profiles for an 80 wt% alumina slurry containing 0.577 wt% CE64 measured at 2300 G.

Further advantages are the low required sample quantity of only 0.5 mL and the opportunity to measure up to 12 samples simultaneously under identical conditions. Results of the optical centrifuge complement conclusions obtained from particle charge titration analyzer and viscometer.

II. Experimental

(1) Materials and preparation

Alumina powder AES-11 (Sumitomo Chemical, Japan) or/and zirconia powder TZ-3YS-E (Tosoh Corporation, Japan) were used in all experiments. For granulation and dry pressing, organic additives Dolapix CE64 (dispersant), Optapix AC 95 (binder) and Zusoplast 9002 (lubricant) all produced by Zschimmer & Schwarz GmbH & Co KG (Germany) were selected and used as received. Optapix AC95 and Zusoplast 9002 were chosen, based on recommendations of the manufacturer stating a special suitability for spray drying. Diluted nitric acid (10.6 wt%) was used to destabilize the slurries.

Aqueous slurries of three different powder batches were prepared: 100 wt% alumina, 100 wt% zirconia and 80 wt% alumina + 20 wt% zirconia, respectively. Grinding bodies (alumina or zirconia balls) and dispersant were added to the suspension fluid (deionized water, 1 μS/cm), followed by the addition of ceramic powder. Mixing and homogenization of the slurry were conducted in a polyethylene container, rotating at 40 rpm for 14 hours. After the grinding bodies had been removed by sieving, binder and lubricant were added using a pipette while the slurry was stirred. For the preparation of destabilized slurries, nitric acid was added last using a pipette.

Granulation via spray drying was carried out in a lab spray dryer (Atomizer Minor, Niro, Denmark). The spray dryer was run in fountain mode with an external mix two-stream nozzle which had a slurry feed orifice diameter of 1.5 mm. The air as atomizing fluid was vortexed within the nozzle by a swirl disc right before the slurry was atomized. Process parameters such as slurry feed rate (17 – 25 mL/min), atomization gas flow rate (38 – 40 L/min), and gas outlet temperature (100 – 105 °C) were kept constant in all spray-drying experiments. For each material (alumina, zirconia, and ZTA), a well-dispersed and a destabilized slurry was spray-dried. Destabilized alumina and zirconia slurries contained 65 wt% solids content, the other slurries contained 70 wt% solids content.

From the spray-dried granules, cylindrical green compacts with a diameter of 20 mm and a height of about 2 mm were pressed with a uniaxial pressure of 100 MPa using a hand-lever press (Paul-Otto Weber GmbH, Germany).

Thermal processes were performed in a box furnace (FHT 16/8, Ceram-Aix, Germany), starting with a slow heating rate of 1 K/min and a dwell time of 30 minutes at 450 °C for debinding. Afterwards, the samples were heated at 5 K/min to the maximum process temperature of 1580 °C for Al_2O_3 and ZTA (60 min dwell time) or 1500 °C for ZrO_2 (30 min dwell time), respectively. A cooling rate of 5 K/min was held up to 300 °C.

(2) Testing procedures

The particle size distribution of the starting powders was determined in aqueous dispersions with a Mastersizer 2000 (Malvern, United Kingdom). Powders were suspended in deionized water and treated with ultrasound for 3 minutes. The test suspensions were cooled to room temperature before the measurement. The specific surface area (BET) was measured based on nitrogen adsorption with a NOVA 2200 (Quantachrome Instruments, USA). Phase content was measured by means of X-ray diffraction (Bruker D8, Germany).

The effectiveness of the dispersant was assessed with zeta potential measurements based on the streaming potential of the ceramic slurries by means of particle charge titration analysis (Stabino, Particle Metrix GmbH, Germany). Suspensions with 20 wt% solids content, the maximum solids content measurable across the whole pH-range, were tested. Although zeta potentials of slurries with a practical solids content of up to 80 wt% are not measurable, conclusions can still be drawn, although they can only be adapted qualitatively. Absolute values of the zeta potential above 30 mV commonly indicate sufficient stabilization [17], but for safe processing a large distance to the isoelectric point (IEP), meaning the point of zero charge where electrostatic stabilization is no longer present, is required additionally.

Sedimentation behavior of well-dispersed and destabilized slurries was monitored and quantified using an optical centrifuge (LUMiSizer©, LUM GmbH, Germany), which allows slurry investigation under centrifugal forces up to 2300 G (rotational speed of 4000 rpm) [18]. For the determination of a suitable dispersant concentration, 80 wt% alumina suspensions with varying dispersant concentrations were measured at maximum rotational speed. Measurements of spray-drying slurries were performed with 2000 rpm (centrifugal force of 530 G) and 30 s time interval between profiles. A well-dispersed alumina slurry with 70 wt% solids content and a destabilized alumina slurry with 65 wt% solids content were investigated.

Slurry viscosity was monitored using a standard rheometer (Physica MCR 300, Anton Paar, Austria). For the spray-drying process, a viscosity below 0.2 Pa·s at a shear rate of 100 s^{-1} was required.

The size distribution of spray-dried granules was measured with a Mastersizer S (Malvern, United Kingdom) using the dispersion unit for dry samples with a feed rate of 20 % and a pressure of 0.16 bar. The shape was determined with a light optical microscope Axiotech 30 (Zeiss; Germany). Flowability measurements and determination of untapped bulk density of granules were conducted in compliance with standards [19, 20] with apparatus conforming to standards (Landgraf Laborsysteme HLL GmbH, Germany).

The green density of the dry-pressed samples was determined by measuring mass and geometry. The sintering density was measured with the Archimedes method [21]. Light optical microscope Axiotech 30 and SEM Gemini Supra 40 (both Zeiss GmbH, Germany) were used for microstructural investigations. Evaluation of sintered body cross-sections in respect of porosity was performed by means of image processing with PxF Workbench software

with phase fraction expansion module (PixelFerber, Germany).

Biaxial strength of four samples per batch was determined with as-fired sintered samples on a ball-on-three-balls (B3B) setup [22,23]. In the B3B-test, one surface of a disc-shaped specimen is supported on three balls equidistant from its center. The opposite face is centrally loaded with a fourth ball normal to the orientation of the plane. The sample holder was used in a testing machine (Zwick/Roell, Germany), which can apply a maximum force of 5 kN. The preload on each specimen was 30 N and the loading rate was 0.03 mm/s.

III. Results and Discussion

Table 1 summarizes results of the characterization of both submicron starting powders. Alumina and zirconia powders are similar in terms of granulometric properties, advantageous for preparation of batches with homogeneous distribution of both components.

Table 1: Properties of alumina and zirconia powders.

Powder properties	Alumina (type AES-11)	Zirconia (type TZ-3YS-E)
Density / g·cm^{-3}	3.94	5.93
Specific surface / m^2·g^{-1}	6.46	6.71
Mean particle size d_{50} / µm	0.58	0.53
Phase content	α-Al_2O_3	tetragonal + low amount monoclinic ZrO_2

(1) Development of slurries with optimum dispersed particles

The results of zeta potential analysis of alumina and zirconia suspensions without any dispersant are shown in Fig. 2. An aqueous suspension with 20 wt% solids content consisting only of the pure raw material delivered a zeta potential of ζ = -31 mV at a pH = 9.3 and an isoelectric point (pH_{IEP}) of 8.6 in case of the used alumina (continuous line in Fig. 2), while pure zirconia delivered ζ = +67 mV at pH = 5.3 and pH_{IEP} of 7.0 (dotted line in Fig. 2). The rather small distances of the IEP from the initial pH-values in case of the dispersing-agent-free suspensions of both raw materials indicate a rather unstable state unsuitable for safe processing despite the sufficiently high absolute zeta potential. Additionally, a well-dispersed and stable multi-component ZTA system consisting of both materials is not possible, since a mixture of both materials would agglomerate owing to the opposite surface charge. Thus, the use of a dispersing agent is inevitable for the ZTA powder.

Comprehensive studies, conducted in a previous research project [24], showed the most promising results regarding sedimentation and slurry viscosity for the commercially available CE64 as dispersing agent. Besides increased absolute zeta potentials, the dispersing agent also shifts the IEP to lower pH-values (Fig. 3). The alumina slurry containing the dispersing agent reaches a ζ = -53 mV at a pH = 9.6 with the IEP now shifted to pH = 5.5. The zirconia even shows a charge reversal, the formerly positive surface became negative, leading to a ζ = -82 mV at a pH = 8.8. The new isoelectric point at pH_{IEP} = 4.9 has a good distance from the initial pH value, similar to the conditions in the alumina slurry.

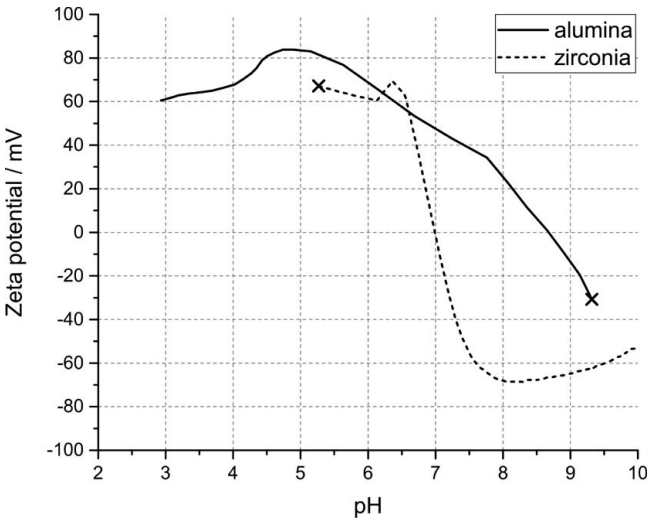

Fig. 2: Starting conditions of both slurries were marked with a black cross. Lines show the evolution of the zeta potential versus the pH for slurries of 20 wt% solids content without dispersing agent for alumina and zirconia.

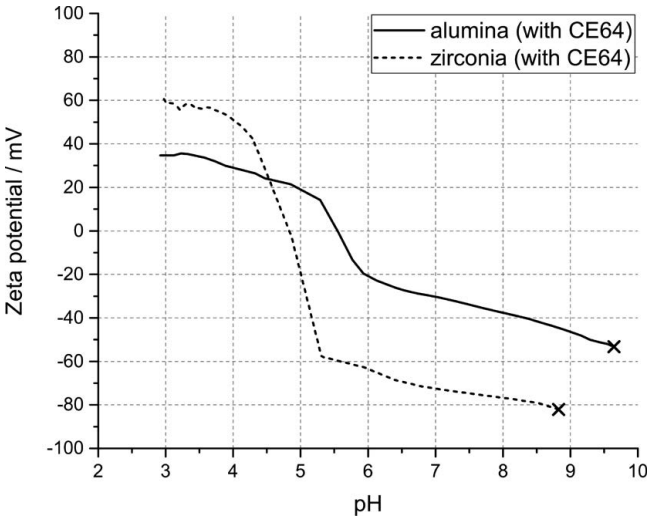

Fig. 3: Starting situation of both slurries marked with black cross and evolution of the zeta potential versus pH for slurries with 20 wt% solids content of alumina and zirconia, both containing 0.577 wt% CE64 with reference to the solid fraction.

The effect of the different dispersant concentrations on sedimentation behavior is shown exemplarily in Table 2. Stated dispersant concentrations refer to the solids content and usage of dispersant as received. The lowest sediment height and the slowest sedimentation velocity, both were observed for a concentration of 0.577 wt% CE64 and indicate the highest degree of dispersion and best stabilization of the powder particles. The active substance amount in the delivered form of 65 % and the fraction of it being citric acid based on investigations of Kosmač *et al.* [25] leads

to a theoretical citric acid content of 0.225 wt%. Therefore, the determined amount with optimal dispersing effect of $1.8 \cdot 10^{-6}$ mol/m^2 is slightly above the adsorption value of $1.2 \cdot 10^{-6}$ mol/m^2, published for a higher-purity alumina [26].

As promising and powerful the centrifugation analysis is, it needs to be accompanied by viscosity measurements, because sufficient stability is not necessarily associated with a processable viscosity below 0.2 Pa·s at a shear rate of 100 s^{-1}, which is required for the spraying process. The addition of 0.577 wt% CE64 again yielded the best result, here the lowest viscosity (dotted line in Fig. 4). Since all tested dispersant concentrations yielded sufficient viscosities at the determined shear rate of 100 s^{-1}, the optimal concentration of 0.577 wt% of dispersant formerly determined by sedimentation analysis, was selected for use in spray slurry preparation.

Since the process route contains a dry pressing step as the shaping procedure, additional binder and lubricating agent are required to achieve stable green bodies. The ideal concentrations were determined via statistical design of experiment yielding the highest sinter density for comparatively low amounts of 1 wt% of binder and 0.5 % of the lubricating agent. Addition of the organic components to the slurry showed a negligible influence on the viscosity. Since the additives have only 50 wt% solids content, the minor effect observed is simply caused by the slight dilution owing to the introduction of water.

The ratio of the organic additives was kept constant for both raw materials to finally apply the optimizations to the multicomponent ZTA material. As result of comprehensive qualitative and quantitative variations, identical organic additives (0.577 wt% dispersant + 1 wt% binder + 0.5 wt% lubricant) were used for preparation of alumina, zirconia and ZTA spray slurries, respectively.

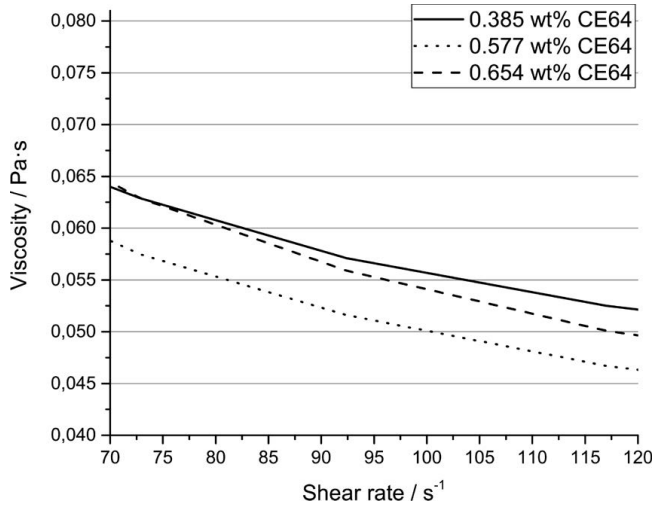

Fig. 4: Viscosity versus shear rate of an 80 wt% alumina slurry with different amounts of CE64 (continuous line 0,385 wt%; dotted line 0,577 wt%; dashed line 0,65 wt%).

(2) Development of destabilized slurries

From the correlation of suspension stability and granule morphology shown in the literature and the influence of suspension stability on the packing density of the sediment in the centrifugation, the conclusion was drawn that the particles' packing behavior in a centrifugation process can qualitatively be transferred to the packing behavior of drying droplets in the spray drying process. Adjustments of the degree of flocculation in ceramic slurries can be achieved by changing either the amount of dispersant or the pH-value. The amount of dispersant is already given, because the slurry preparation needed the dispersing agent to homogeneously disperse and afterwards stabilize the particles. Furthermore, the dispersing agent is necessary to achieve the required high solids content and the surface charge reversal of the zirconia material. With the dispersant amount fixed, the option left for a defined destabilization leading to a specific flocculation is the adjustment of the slurry's pH.

Table 2: Sediment height and sedimentation velocity in an 80 wt% alumina slurry depending on dispersing agent concentration of CE64 at 4000 rpm (2300 g).

Concentration of dispersing agent / wt%	Relative sediment height / %	Sedimentation velocity / µm·s^{-1}
0.385	77.4	5.6
0.577	75.5	4.7
0.654	76.0	4.9
0.769	76.5	5.2

The optical centrifuge was used for the determination of the necessary amount of nitric acid to reach a specific degree of flocculation. The required degree of flocculation is reached when the slope of the individual transmission profile is nearly vertical. The reduction of the pH and approaching the IEP was realized by the addition of diluted nitric acid (10.6 wt%). Results of sedimentation analysis are depicted in Fig. 5 and show an increase in the sedimentation rate (increased distance between transmission profiles). Assessing the relative sediment heights, it needs to be noted that the recorded spectrum at the bottom (Fig. 5) is of a slurry with only 65 wt% solids content (reduced by 5 wt% compared to the measurement shown on top of Fig. 5) and still leads to sediment that is nevertheless higher. The destabilized 65 wt% slurry yields a relative sediment height of 68.3 % while the dispersed 70 wt% slurry yielded a relative sediment height of 64.8 %.

The higher final relative sediment height achieved indicates a less dense packing in the cuvette in the case of acid addition. This higher final relative sediment height by reduction in packing density even overrules the lower overall filling height and reduced solids content. So, this destabilization leads to a pronounced reduction in packing density. The reduced packing density enables shrinking of the atomized droplet during drying and therefore maintenance of its spherical shape.

The apparently narrow particle size distribution indicated by the vertical slope of the transmission profiles in the spectrum of the destabilized slurry is the result of a network structure established in the slurry. The desired degree of flocculation for alumina is achieved for a pH value

of approximately pH = 8. The pH shift leads to a generation of charges on the particle surface and the formerly optimized weight ratio of the dispersant becomes insufficient. The generated unsaturated surface charges are attracting dispersant molecules even though they might already be bound to another particle. These bridging connections [27] of dispersant molecules lead to a network formation and therefore defined partial flocculation in the destabilized system.

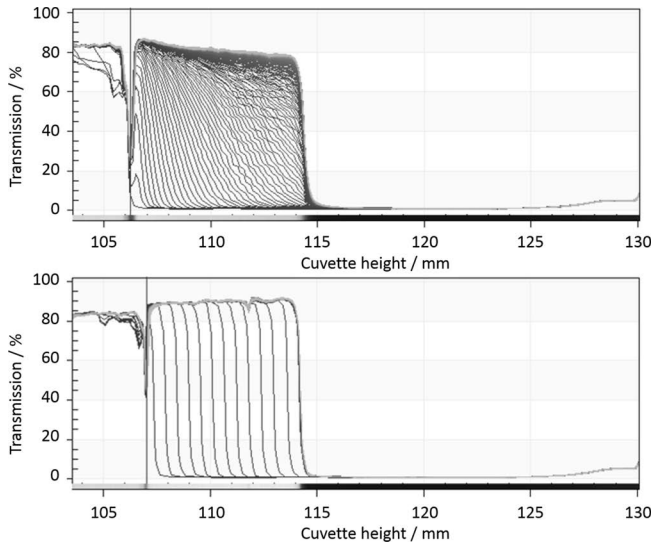

Fig. 5: Effect of the destabilization on the sedimentation behavior. The images show the transmission profiles of a dispersed 70 wt% (top) and destabilized 65 wt% (bottom) alumina, both slurries contain 0.577 wt% CE64. (measured at 2000 rpm; 530 G).

In the case of alumina, the required amount of nitric acid was V_{acid} = 14.9 µL/g (additions refer to the powder mass), while the zirconia slurry only needed V_{acid} = 9.0 µL/g. The pH required for the desired degree of flocculation for both raw powder materials is in the range marked in Fig. 6 and therefore, applicable as well as for the ZTA composite. The ZTA slurry required V_{acid} = 12.0 µL/g for sufficient destabilization.

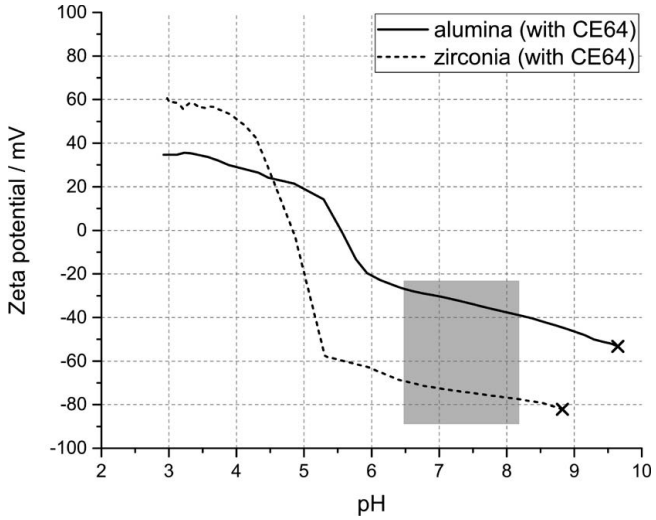

Fig. 6: The plot shows zeta potential versus pH for slurries containing CE64, indicating the process window of flocculated slurries (gray area) and their initial pH values (black crosses) for alumina and zirconia.

Further acid addition and therefore increased flocculation of the slurry does not lead to an improvement of properties. The stabilization sustained in the case of the defined flocculation is lost and the slurry completely flocculates. Thereby, slurry viscosity increases and safe slurry processing cannot be assured. Since shrinkage of the atomized droplets leading to bulky soft granules is already possible in partially destabilized slurries, there is no necessity for further flocculation. With the defined flocculation realized, the viscosity rose to values above the workable limit of η = 0.2 Pa·s at a shear rate of 100 s^{-1}. The parameters strongly affecting the viscosity are dispersant concentration and the solids content. Since the desired flocculation is based on impoverishment of the dispersant, the second major influencing factor needed adjustment. The solids content had to be reduced to maintain or regain a processable range of the viscosity. The required viscosity was achieved by reducing the solids content of the pure powder slurries (alumina and zirconia) to 65 wt%. The dependence of the viscosity on the solids content is shown by way of example for alumina in Fig. 7. The well-dispersed slurry appears as a flat base line (depicted as a dashed line in Fig. 7) compared to the destabilized slurries. The viscosity of the 70 wt% destabilized slurry (dotted line) is too high for the upcoming atomization process, while the 65 wt% destabilized slurry (continuous line) regains suitable viscosity and was further used for the subsequent spray drying procedure.

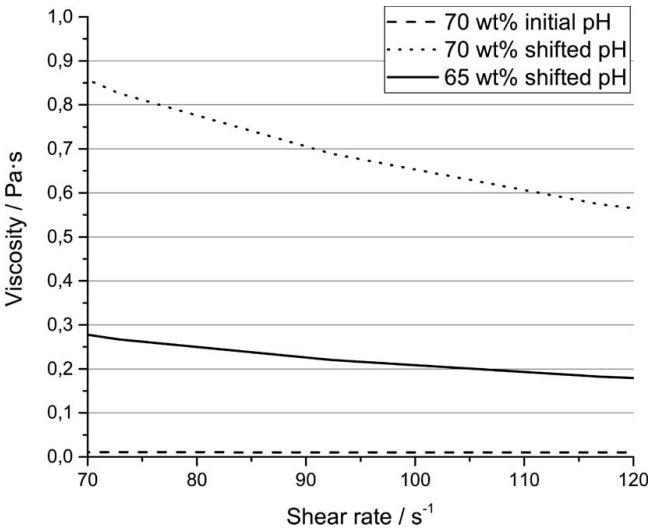

Fig. 7: Effect of pH adjustment on slurry viscosity as an example for alumina slurries.

(3) Spray drying and green body characterization

All slurries were atomized with a two-fluid nozzle using pressurized air. Table 3 lists the solids content, the pH-values of slurries and the corresponding granulate yield of all batches produced from dispersed and destabilized slurries, respectively. The given granule yield is the coarser fraction produced in the spraying process. The fine dust-like fraction is not included in the granulation yield since it is unsuitable for dry pressing processes. The process yield is only slightly affected by the destabilization of the slurry without an explicit tendency.

Granules made of well-dispersed slurries show the typical morphology for spray-dried granules, with one side of the granule curved inwards (dimple), resembling a kicked-in football. The irregular granules made of well-dispersed slurries of the different materials are depicted in the top row of Fig. 8. The irregular shape seems not to depend on the granules' size. The dimpled shape can be found over the whole granule size range.

In contrast, granules made of the destabilized slurries show in all cases a reduced fraction of dimpled particles and are depicted in Fig. 8 d) – f) for all three materials.

Table 4 gives an overview regarding the different granule properties. The size distribution of the granules is differently affected by destabilization for the different materials. The size of granules prepared from destabilized slurries compared to stable slurries is slightly decreased for alumina, strongly decreased for zirconia, but strongly increased for ZTA. The granule flowability depends on the granule size and increases with increasing granule diameter. Thus, destabilization of alumina and zirconia slurries reduces the granule flowability by 18.5 % and 54.5 %, respectively. In the case of ZTA, slurry destabilization improves granule flowability by 6.9 %. This observed correlation between flowability and particle size is in agreement with investigations already described in the literature [1]. The untapped bulk density of the granules is reduced by the slurry destabilization as the destabilization prevents a dense packing in the drying step.

Table 3: Characteristics of the spray drying experiments.

Batch name	Solids content / wt%	pH	Granulate yield / %
Al_{disp}	70	9.5	44
Zr_{disp}	70	9.1	62
ZTA_{disp}	70	9.5	58
Al_{destab}	65	7.8	42
Zr_{destab}	65	6.6	62
ZTA_{destab}	70	8.3	47

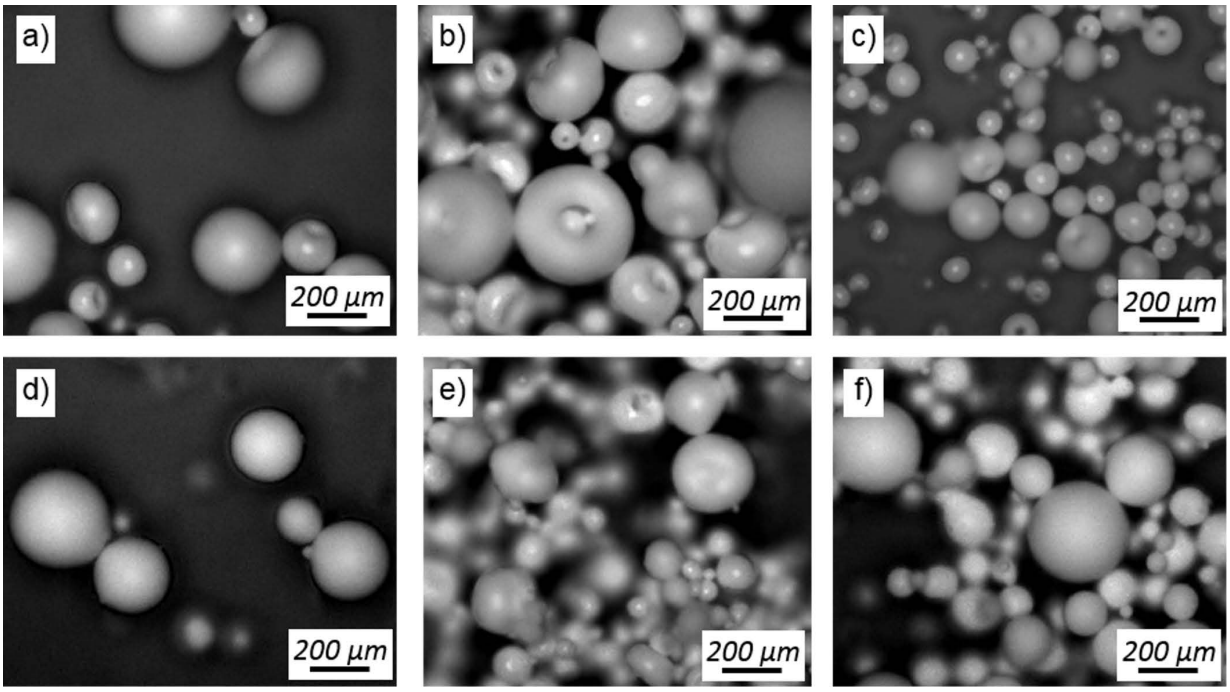

Fig. 8: Light microscope images of granules of alumina (a and d), zirconia (b and e) and ZTA (c and f) from slurries with well-dispersed particles (a - c) and destabilized slurries (d - f).

Table 4: Characteristics of granules and pressed compacts produced by dispersed and destabilized slurries.

	Al_{disp}	Al_{dest}	Zr_{disp}	Zr_{dest}	ZTA_{dis}	ZTA_{dest}
Granules d_{10} / µm	16	11	16	7	15	19
Granules d_{50} / µm	53	42	50	27	49	74
Granules d_{90} / µm	132	118	118	65	112	170
Granules' flowability / $g \cdot s^{-1}$	0.81	0.66	1.23	0.56	0.87	0.93
Granules' untapped bulk density / $g \cdot cm^{-3}$	1.25	1.10	1.60	1.43	1.32	1.23
Pressed compacts' green density / $g \cdot cm^{-3}$	2.23	2.20	2.86	2.83	2.37	2.31

Despite large differences in granules untapped bulk density, the granule compactibility is only slightly affected by slurry destabilization. Sample body preparation by dry pressing of granules made of destabilized slurries leads to green bodies with a slightly reduced density compared to sample bodies of granules from well-dispersed slurries.

An important difference in the fabricated sample bodies can be observed when green sample bodies are broken. Evaluating the fracture surface, the sample body made of granules from a dispersed slurry shows round, sphere like residues of the granules (depicted exemplarily for alumina in the left image of Fig. 9). In contrast, no sphere-like granule residues are obvious at the fracture surface of the green body made from destabilized slurry. The crack does not propagate along the borders of maintained granules, but instead randomly through the granule volume (right image in Fig. 9), indicating soft granules without hollow cores and hard shells.

(4) Sintered body properties

Sintered bodies produced with granules from well-dispersed slurries show overall a higher number of pores compared to sintered bodies made with granules of destabilized slurries (Fig. 10). The reduction in pore number and size was observed for all three materials. The pore area in these microstructure images was determined (Table 5) and supports this finding with a pore fraction reduction in the sintered bodies originating from destabilized slurries to approximately one third compared to sinter bodies originating from well-dispersed slurries.

As shown in Fig. 10, the sintered bodies originating from destabilized slurries, show a more dense and homogeneous microstructure. This trend is expressed in the sintered body density, too. For all investigated materials, the sintered bodies originating from destabilized slurries yield a higher density, which is listed in Table 5.

Results of biaxial strength measurements for the different materials are listed in Table 5 and shown in Fig. 11. In all cases, the sintered bodies (originating from destabilized slurries) show higher values for the mean strength as well as for the minimal strength, but these improvements should be considered as a tendency. Zirconia shows a particularly strong increase but an increased standard deviation as well.

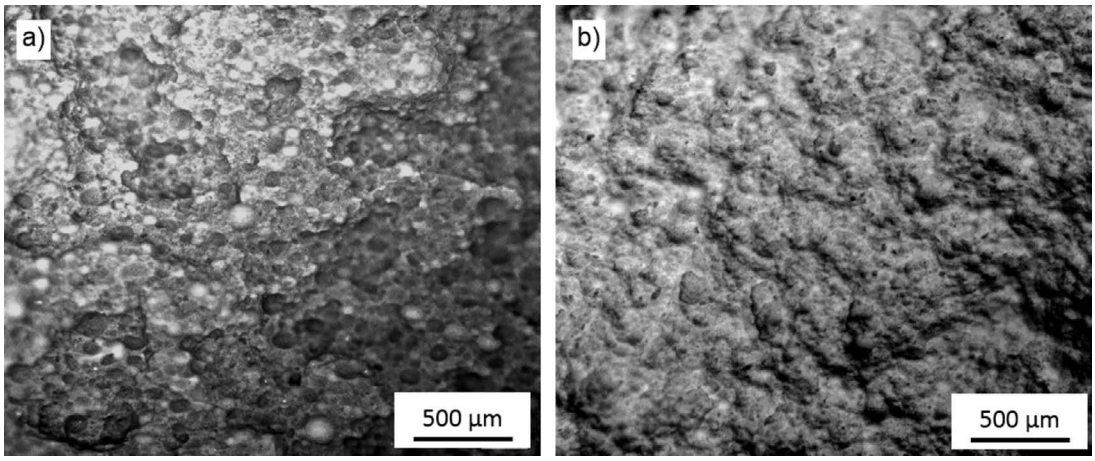

Fig. 9: Light images of fracture areas of alumina green samples made of granules from the dispersed slurry (a) and destabilized slurry (b).

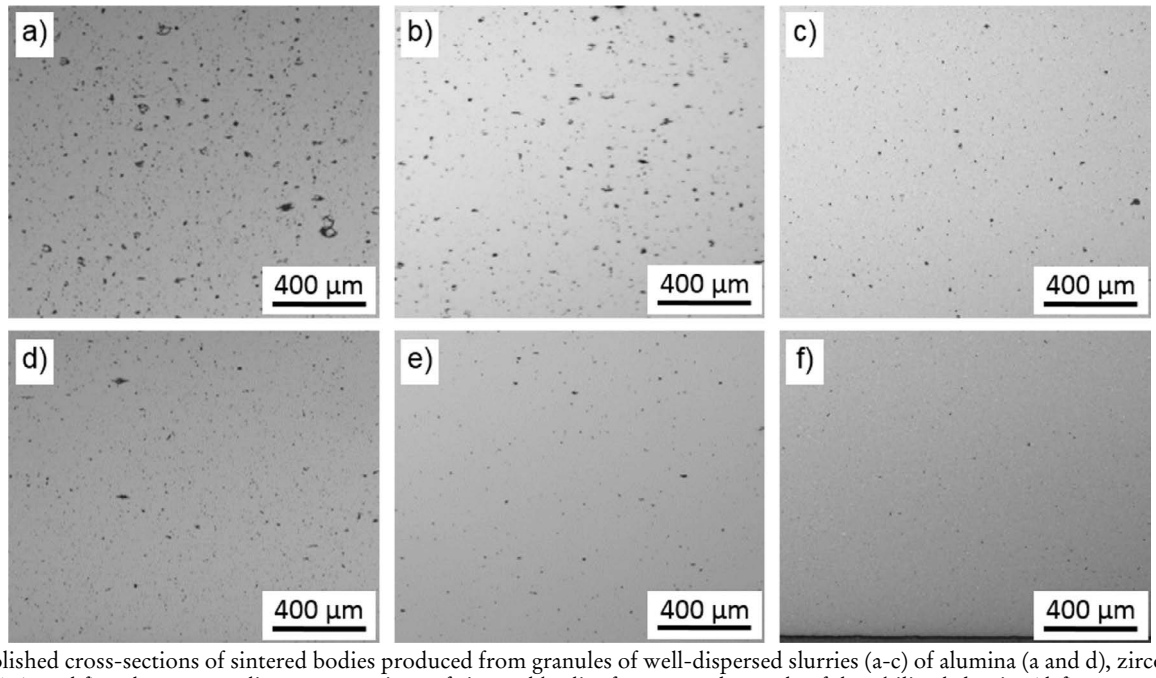

Fig. 10: Polished cross-sections of sintered bodies produced from granules of well-dispersed slurries (a-c) of alumina (a and d), zirconia (b and e) and ZTA (e and f) and corresponding cross-sections of sintered bodies from granules made of destabilized slurries (d-f).

Table 5: Characteristic values of sintered alumina, zirconia and ZTA bodies, made of the differently treated slurries

	Al_{disp}	Al_{dest}	Zr_{disp}	Zr_{dest}	ZTA_{dis}	ZTA_{dest}
Porosity / %	4.0	1.4	2.8	1.2	1.4	0.5
Sintered density / g·cm^{-3} with standard deviation	3.863 ± 0.008	3.882 ± 0.005	5.962 ± 0.010	5.992 ± 0.002	4.172 ± 0.001	4.183 ± 0.004
Mean strength / MPa and standard deviation / %	409 ± 10.8 %	498 ± 11.6 %	518 ± 5.6 %	818 ± 25.3 %	603 ± 17.1 %	644 ± 15.6%
Minimal strength / MPa	348	427	493	563	487	519

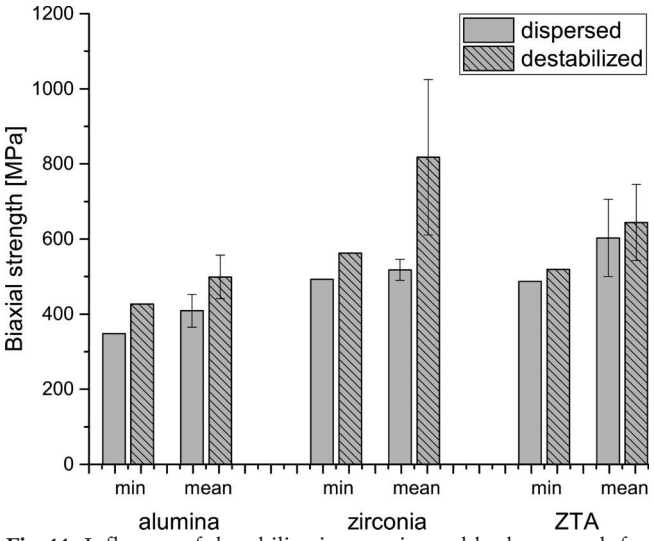

Fig. 11: Influence of destabilization on sintered body strength for alumina, zirconia and ZTA.

IV. Summary

The influence of the initial slurry stability on the properties of granules, green and sintered bodies has been investigated for alumina, zirconia and ZTA composite materials.

Zeta potential and viscosity measurements as well as sedimentation investigations with optical centrifuge were used for precise slurry assessment as a major precondition for optimum and reproducible adjustment of slurries before spray drying. Sedimentation analysis with optical centrifuge (LUMiSizer©) has been used to investigate different influences like additive composition, solids content or pH-value on the sedimentation behavior. Granules were prepared from well-dispersed and destabilized slurries. The prepared granules have been used to fabricate green bodies which were subsequently sintered.

Granules produced by spray drying of well-dispersed slurries have the donut like morphology that is common and well known for conventional, commercially available granules. Spray drying of destabilized slurries leads to a lower granule bulk density and a strongly decreased fraction of granules with a disadvantageous hard shell and donut-like morphology. Typical inhomogeneities in the microstructure as they result from hollow granule cores or hard granule shells were found in dry-pressed, and afterwards broken, green sample bodies. In contrast, such inhomogeneities were not observed in broken green bodies made of granules of destabilized slurries. Sintered sample bodies based on the specifically destabilized slurries exhibited a higher sintered density, reduced pore fraction, reduced maximum pore size and increased biaxial strength compared to sintered bodies from conventional well-dispersed slurries. The efficacy of the strategy to improve the microstructure and strength of green and sintered bodies by precisely adjusting the initial slurry stability has been proven for single-component ceramics (alumina and zirconia) as well as for multicomponent ceramic materials (ZTA).

Acknowledgements

The authors would like to thank the Federal Institute for Economic Affairs and Energy (Germany) and the Central Innovation Programme for SMEs for financial support (grant KF2201088AG4). Further, we should like to thank Wolfgang Güther (BAM Division 5.5) for his extensive support with spray drying and sample preparation, Franziska Lindemann (BAM Division 5.5) for powder and sample body characterization and Dagmar Nicolaides (BAM Division 5.4) for biaxial strength measurements.

References

1 German, R.M.: Particle Packing Characteristics, Metal Powder Industries Federation: Princeton New Jersey, (1989).

2 Zhang, Y., Binner, J., Rielly, C., Vaidhyanathan, B.: Comparison of spray *freeze* dried nanozirconia granules using ultrasonication and twin-fluid atomisation, *J. Eur. Ceram. Soc.,* **34**, [4], 1001 – 1008, (2014).

3 Rosenberger, N., Compson, C., Adria, J.: Comparative study on lab-scale granulation techniques, cfi *Ber. DKG,* **92**, [4], E29 – E31, (2015).

4 Shinohara, N., Okumiya, M., Hotta, T., Nakahira, K., Naito, M., Uematsu, K.: Morphological changes in process-related large pores of granular compacted and sintered alumina, *J. Am. Ceram. Soc.,* **83**, [7], 1633 – 1640, (2000).

5 Vicente, J., Pinto, J., Menezes, J., Gaspar, F.: Fundamental analysis of particle formation in spray drying, *Powder Technol.,* **247**, 1 – 7, (2013).

6 Baklouti, S., Chartier, T., Baumard, J.F.: Binder distribution in spray-dried alumina agglomerates, *J. Eur. Ceram. Soc.,* **18**, [14], 2117 – 2121, (1998).

7 Tanaka, S., Pin, C.C., Uematsu, K.: Effect of organic binder segregation on sintered strength of dry-pressed alumina, *J. Am. Ceram. Soc.,* **89**, [6], 1903 – 1907, (2006).

8 Lee, H.-W., Song, G., and Suk, I.-S.: Effect of suspension property on granule morphology and compaction behavior, pp. 41 – 50 in 96. annual meeting of the American Ceramic Society (ACS). (1995).

9 Takahashi, H., Shinohara, N., Okumiya, M., Uematsu, K., Junichiro, T., Iwamoto, Y., Kamiya, H.: Influence of slurry

flocculation on the character and compaction of spray-dried silicon-nitride granules, *J. Am. Ceram. Soc.,* **78**, [4], 903 – 908, (1995).

10 Bertrand, G., Filiatre, C., Mahdjoub, H., Foissy, A., and Coddet, C.: Influence of slurry characteristics on the morphology of spray-dried alumina powders, *J. Eur. Ceram. Soc.,* **23**, [2], 263 – 271, (2003).

11 Tsubaki, J., Yamakawa, H., Mori, T., Mori, H.: Optimization of granules and slurries for press forming, *J. Ceram. Soc. Japan,* **110**, [10], 894 – 898, (2002).

12 Walker, W.J., Reed, J.S., Verma, S.K.: Influence of slurry parameters on the characteristics of spray-dried granules, *J. Am. Ceram. Soc.,* **82**, [7], 1711 – 1719, (1999).

13 Mahdjoub, H., Roy, P., Filiatre, C., Bertrand, G., Coddet, C.: The effect of the slurry formulation upon the morphology of spray-dried yttria stabilised zirconia particles, *J. Eur. Ceram. Soc.,* **23**, [10], 1637 – 1648, (2003).

14 Cao, X.Q., Vassen, R., Schwartz, S., Jungen, W., Tietz, F., Stoever, D.: Spray-drying of ceramics for plasma-spray coating, *J. Eur. Ceram. Soc.,* **20**, [14 – 15], 2433 – 2439, (2000).

15 Kim, D.J., Jung, I.Y.: Granule performance of zirconia/alumina composite powders spray-dried using polyvinyl pyrrolidone binder, *J. Eur. Ceram. Soc.,* **27**, [10], 3177 – 3182, (2007).

16 Naglieri, V., Gutknecht, D., Garnier, V., Palmero, P., Chevalier, J., Montanaro, L.: Optimized slurries for spray Drying: different approaches to obtain homogeneous and deformable alumina-zirconia granules, *Materials,* **6**, [11], 5382 – 5397, (2013).

17 Greenwood, R.: Review of the measurement of zeta potentials in concentrated aqueous suspensions using electroacoustics, *Adv. Colloid Interfac.,* **106**, [1], 55 – 81, (2003).

18 Lerche, D., Sobisch, T.: Evaluation of particle interactions by in situ visualization of separation behaviour, *Colloid Surface A,* **440**, 122 – 130, (2014).

19 EN ISO 14629:2016 (German version); Fine ceramics (advanced ceramics, advanced technical ceramics) - Determination of flowability of ceramic powders (ISO 14629:2012); in CEN, Brussels, 2016.

20 EN 725 – 9:2006 (German version); Advanced technical ceramics – Methods of test for ceramic powders - Part 9: Determination of untapped bulk density (EN 725 – 9:2006); in CEN, Brussels, 2006.

21 EN 623 – 2 Advanced technical ceramics - Monolithic ceramics - General and textural properties - Part 2: Determination of density and porosity. in CEN, Brussels, 1993.

22 Borger, A., Supancic, P., Danzer, R.: The ball on three balls test for strength testing of brittle discs: Part II: Analysis of possible errors in the strength determination, *J. Eur. Ceram. Soc.,* **24**, [10 – 11], 2917 – 2928, (2004).

23 Danzer, R., Harrer, W., Supancic, P., Lube, T., Wang, Z. H., Borger, A.: The ball on three balls test - strength and failure analysis of different materials, *J. Eur. Ceram. Soc.,* **27**, [2 – 3], 1481 – 1485, (2007).

24 Final Report of ZIM Project: Ultrasonic supported, energy-efficient spray granule synthesis, Support code KF2201088, BAM Berlin, (2016).

25 Aleš, D., Tomaž, K.: Weakly flocculated aqueous alumina suspensions prepared by the addition of Mg(II) ions, *J. Am. Ceram. Soc.,* **83**, [3], 666 – 668, (2000).

26 Hidber, P.C., Graule, T.J., Gauckler, L.J.: Competitive adsorption of citric acid and Poly(vinyl alcohol) onto alumina and its influence on the binder migration during drying, *J. Am. Ceram. Soc.,* **78**, [7], 1775 – 1780, (1995).

27 Shojai, F., Pettersson, A.B.A., Mäntylä, T., Rosenholm, J.B.: Electrostatic and electrosteric stabilization of aqueous slips of 3Y-ZrO_2 powder, *J. Eur. Ceram. Soc.,* **20**, [3], 277 – 283, (2000).